

GOLD NANOPARTICLES IN CANCER CELL LINES

IGNÁC CAPEK

Slovak Academy of Sciences, Polymer Institute, Institute of Measurement
Sciences, Dúbravská cesta, Bratislava, Slovakia

ABSTRACT

Gold nanoparticles have immense potential for cancer diagnosis and therapy on account of their light absorption and scattering. Conjugation of gold nanoparticles (AuNPs) to ligands specifically targeted to biomarkers on cancer cells allows molecular-specific imaging and detection of cancer. The development of smart AuNPs that can deliver therapeutics at a sustained rate directly to cancer cells may provide better efficacy and lower toxicity for treating cancer tumors. Using targeted nanoparticles to deliver chemotherapeutic agents in cancer therapy offers many advantages to improve drug/gene delivery and to overcome many problems associated with conventional chemotherapy. AuNPs efficiently convert the absorbed light into localized heat, which can be exploited for the selective laser photothermal therapy of cancer.

KEYWORDS: Gold Nanoparticles, Drug Delivery, Tumors, Cancer Therapy

INTRODUCTION

Cancer Image

Targeted therapies are a major focus of cancer research today. With recent advances of nanotechnology, nanoparticle-based targeted drug delivery, especially for cancer therapies, has attracted increasing attention in the past two decades. Nanoparticles have several advantages for targeted drug delivery. First, they are small in size and can escape the uptake of mononuclear phagocytic system (MPS) cells in the blood and organs. Second, the advantages of tumor targeting and controlled drug release often result in increased therapeutic efficacy of the antitumor agents, and weakened side effects [1], whereas most free anticancer drugs are taken up nonspecifically by all types of cells, resulting in serious side-effects. In addition, noble metal nanoparticles are particularly well-suited for crossing various biological barriers, such as leaky vasculature. This approach uses the unique properties of the tumor microenvironment, most notably: (i) leaky tumor vasculature, which is highly permeable to macromolecules relative to normal tissue; and (ii) a dysfunctional lymphatic drainage system, which results in enhanced fluid retention in the tumor interstitial space [2]. As a result of these characteristics, the concentration of polymeric nanoparticles and macromolecular assemblies found in tumor tissues can be up to 100x higher than those in normal tissue [2].

The lymph system of tumours is poorly operational and macromolecules leaking from the blood vessels accumulate - a phenomenon known as “enhanced permeability and retention (EPR) effect” [3]. It has been shown that entities in the order of hundreds of nanometre in size can leak out of the blood vessels and accumulate within tumours. However, large macromolecules or nanoparticles could have limited diffusion in the extracellular space [4]. Experiments from animal models suggest that sub-150 nm, neutral or slightly negatively or positively charged entities can move through tumour tissue [5,6]. However these nanoparticles will be restricted from exiting normal vasculature (that requires sizes less than 1–2 nm); however they will still be able to access the liver, as entities up to 100–150 nm in diameter are able to do so.

Although proliferating endothelial cells are a common hallmark of angiogenic microvascular sprouts, extensive sprouts can grow for periods of time, mainly by the migration of endothelial cells [7]. Physiological angiogenesis is distinct from arteriogenesis and lymphangiogenesis and occurs in reproduction, development and wound repair. It is usually focal, such as in blood coagulation in a wound, and self-limited in time, taking days (ovulation), weeks (wound healing) or months (placentation). By contrast, pathological angiogenesis can persist for years. Pathological angiogenesis is necessary for tumours and their metastases to grow beyond a microscopic size and it can give rise to bleeding, vascular leakage and tissue destruction. These consequences of pathological angiogenesis can be responsible, directly or indirectly, for the symptoms, incapacitation or death associated with a broad range of ‘angiogenesis-dependent diseases’ [8]. Examples of such diseases include cancer, autoimmune diseases, age-related macular degeneration and atherosclerosis. These molecules regulate the proliferative and invasive activity of the endothelial cells that line blood vessels. Some of the most prominent angiogenesis stimulatory molecules include vascular endothelial growth factor (VEGF), basic fibroblast growth factor, platelet-derived growth factor and certain matrix metalloproteinases (Figure 1).

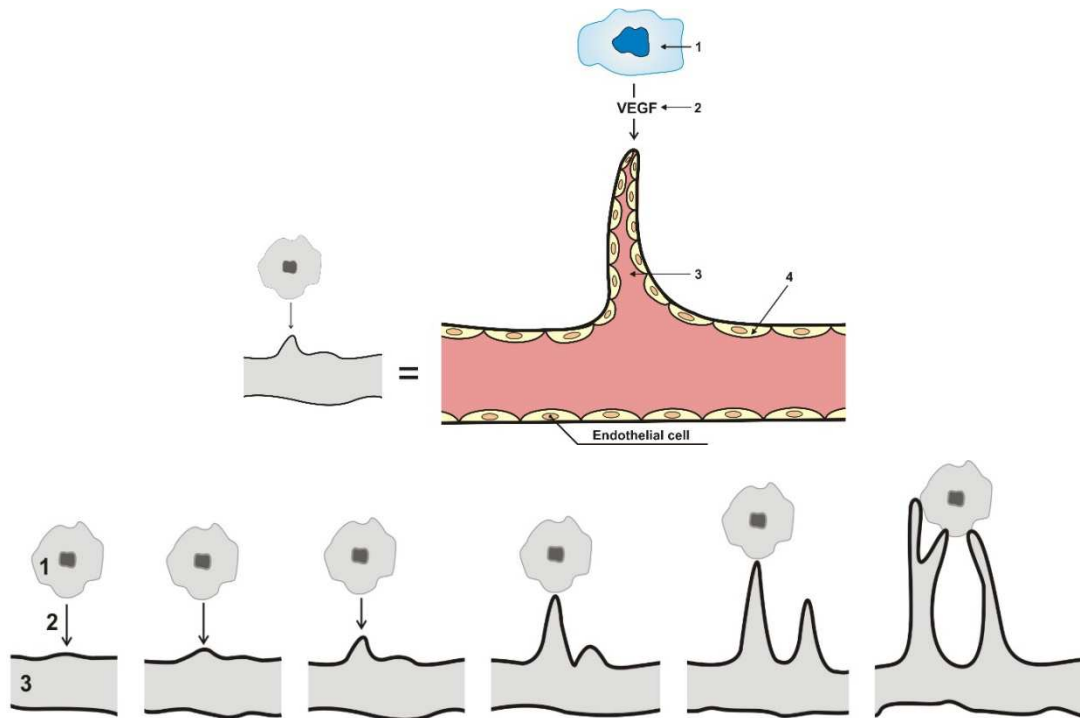


Figure 1

Figure 1. | Angiogenesis and vascularization mechanisms; tumour expression (1) of an angiogenic factor, an angiogenic factor after its secretion from a tumour and an endothelial cell receptor. VEGF (2), vascular endothelial growth factor. Continued tumor development beyond diffusion-limited maximal size. In (B), the angiogenic switch has occurred creating an imbalance of positive to negative regulators causing endothelial cell proliferation and migration. These endothelial cells (4) form a vessel which extends towards the tumor and provides nutrients to sustain cell proliferation. A fully vascularized tumor is capable of continued growth with metastatic potential due to the proximity to the blood stream (3) [9, 10].

Angiogenesis and vascularization are well-characterized for tumors [11]. In tumors, blood vessel walls become leaky because of defective vascular architecture, including poorly aligned endothelial cells with wide fenestrations and a lack of a smooth muscle layer. These properties result from rapid angiogenesis or vascularization because tumor cells

develop so fast and demand a large supply of nutrients and oxygen [12]. The vascular permeability of tumor tissues can also be enhanced by the actions of secreted factors such as kinin and vascular endothelial growth factor [13, 14]. Furthermore, tumor tissues usually lack effective lymphatic drainage. Therefore, macromolecules or leukocytes can be drained through the leaky blood vessels and be retained. This phenomenon was defined as EPR effect [3, 15]. As a result of such increased vascular permeability, particles ranging from 50 to 500 nm in size can be selectively delivered to tumor tissue [16, 17]. When these particles are loaded with anticancer drugs, the therapeutics could be selectively delivered to the tumor tissue [18]. In contrast, very small nanoparticles (<20-30 nm in diameter) can easily pass through the leaky capillary wall in the tumor but can also be returned to circulating blood by diffusion [19]. Therefore, small particles have good permeability but poor retention. However, after conjugation with a targeting ligand, their retention in the tumor could be greatly enhanced [20]. For tumor targeted drug delivery systems, EPR-effect is now widely accepted as a guiding principle [21].

Nanoscale gold particles show great potential as photothermal therapy agents. At sizes larger than ~5 nm, the general assumption is that gold is chemically inert like the bulk. However, the chemical reactivity of gold particles for diameters less than 3 nm is most likely different than both organogold complexes [22] and larger gold nanoparticles [23]. It was found that 50 nm transferrin-coated gold nanoparticles were taken up by mammalian cells at higher rates and extents compared to smaller and larger sizes in the range of 10–100 nm [24]. The explanation of this optimal size was based on the so-called “wrapping effect”, which describes how a cellular membrane encloses nanoparticles. Two factors dictate how fast and how many nanoparticles enter the cellular compartment via “wrapping”: the first is the free energy that results from ligand–receptor interaction; the second is the receptor diffusion kinetics onto the wrapping sites on the cellular membrane. Considering the contribution of these factors and using mathematical calculations, [25] suggested that nanoparticles with 27–30 nm diameter would have that fastest wrapping time and thus the fastest receptor-mediated endocytosis.

Nanoparticle Conjugates

Nanoparticles that are sterically stabilized (for example by poly(ethylene glycol) (PEG) polymers on their surface) and have surface charges that are either slightly negative or slightly positive tend to have minimal self–self and self–non-self interactions. Also, the inside surface of blood vessels and the surface of cells contain many negatively charged components, which would repel negatively charged nanoparticles. As the surface charge becomes larger (either positive or negative), macrophage scavenging is increased and can lead to greater clearance by the reticulo-endothelial system. Thus, minimizing nonspecific interactions via steric stabilization and control of surface charge helps to prevent nanoparticle loss to undesired locations.

Gold nanoparticles with their “special” surface chemistries/arrangements can enter cells by direct penetration [26]. AuNPs (~5 nm) decorated with two capping molecules (anionic and hydrophobic, with alternating positions on the surface) enter the cells directly (endocytosis-independent entry) without destruction to the cell membrane in an action similar to the cell-penetrating peptides. The gold nanoparticles are able to enter cells and are trapped in vesicles, but are not able to enter the nucleus [27]. Using TEM, Nativo et al. showed that 16 nm citrate-capped gold nanoparticles enter cells readily (incubation time 2 h) and are trapped into endosomes. They did not find free nanoparticles in the cytosol or the nucleus. However, they were able to deliver the nanoparticles to the cytosol and nucleus by modifying these nanoparticles with cell-penetrating and nuclear-localizing peptides [28]. AuNPs with especially surface functionalized represent smart and promising candidates in the drug delivery applications due to their unique dimensions, tunable functionalities on the

surface and controlled drug release [29]. Biologically synthesized and functionalized, AuNPs provide many desirable attributes for use as carriers in drug delivery systems as the functionalized AuNP core is essentially inert and nontoxic [30].

Due to a straightforward synthesis, stability, and ease of incorporation of functional groups for targeting capabilities, gold nanomaterials have great application in gene, drug and protein delivery, biological imaging, cancer treatments, and in implants [31]. Particles with longer circulation times, and hence greater ability to target to the site of interest, should be 100 nm or less in diameter and have a hydrophilic surface in order to reduce clearance by macrophages [32]. Coatings of hydrophilic polymers can create a cloud of chains at the particle surface which will repel plasma proteins and work in this area began by adsorbing surfactants to the nanoparticles surface.

Polymeric nanoshells consist of diblock copolymers that can be assembled into a gold composite structure. In general, nanoshells are made by self-assembly of oppositely charged polymers covering the surface of the drug NPs. Therefore, the drug release rate is controlled by the chemistry of the polymers and the diffusion coefficient through the polymeric layer. For example, nanoshells encapsulating doxorubicin have been synthesized using amphiphilic tercopolymer based on polyacrylamide and undecenoic acid derivatives that can trigger intracellular doxorubicin release at pH 6.6. Furthermore, these composite nanoparticles possess a highly tunable plasmon resonance mediated by the size of the core and the thickness of the shell, which in turn determines their absorbing and scattering properties over a broad range of the spectrum from the near-ultraviolet to the mid-infrared [33]. Au nanoshells have been developed for in vivo photothermal therapy using near-infrared light. Gold nanoshell particles with a magnetic core have also been developed for controlled release of 5-fluorouracil [34]. The combination of magnetic particle domains with a drug-encapsulated biodegradable polymer allows for particle targeting to specific sites of the body in response to an externally applied magnetic field.

Target cell-specific aptamers have the potential to serve as molecular probes for specific recognition of the cancerous cells, but unfortunately, aptamers have weak binding affinity and thus gives low signal in molecular imaging, limiting their ability for highly sensitive detection of cancer cells [35]. Conjugating aptamers to nanoparticles has shown to result in more efficient targeted therapeutics or selective diagnostics than nontargeted NPs. Farokhzad et al. have developed NP-aptamer (NP-Apt) conjugates that target the prostate specific membrane antigen (PSMA) [36], a transmembrane protein that is upregulated in a variety of cancers, using the A10 aptamer. This formulation has been further evaluated in vivo in a tumor model of LNCaP prostate cancer cells, which express PSMA antigens, and has been shown to regress tumor size effectively [36(38)]. These authors have also shown that docetaxel delivered using the NP-Apt is more efficacious than nontargeted docetaxel therapy. Bagalkot et al. [37] has also demonstrated a novel strategy for the targeted delivery of anthracycline agents including doxorubicin directly to cancer cells through the formation of an aptamer-doxorubicin physical conjugate. Other labs have also embraced the potential of NP-Apt technologies, including a report of colorimetric assays to detect the presence of platelet-derived growth factor (PDGF) and its receptor using AuNP-Apt conjugates [38].

Specifically, gold nanoclusters of 1.4 nm have been shown to selectively and irreversibly bind to the major grooves of B-DNA and cause increased cytotoxicity compared to larger particles (18 nm). The lack of interaction of larger particles with DNA is suggested to be due to steric hindrance. While gold nanoclusters may be very effective cancer treatments, healthy cells would also be affected potentially causing toxicity [23, 39]. Similarly, Pan et al. studied the size-dependent cytotoxicity of AuNPs (water soluble and stabilized with triphenylphosphine derivatives) on several

different cell lines. They discovered that nanoclusters of 1.4 nm exhibited increased cytotoxicity (IC_{50} = 30 and 46 μ M), whereas nanoclusters of 0.8, 1.2, and 1.8 nm were four to six-fold less toxic. Larger sizes (15 nm) exhibited no cytotoxicity even at high concentrations (6.3 mM) [40]. Moreover, Chithrani et al. examined the uptake of 14, 50, and 74 nm sized citric acid ligand stabilized gold nanoparticles into HeLa cells and determined that 50-nm spheres were more quickly taken up by endocytosis than both the smaller and larger sizes [24]. They further studied the rate of exocytosis of transferrin-coated gold nanoparticles and determined that the rate of exocytosis was size-dependent with more accumulation of larger gold nanoparticles in the cell [41]. When studying the effect of gold nanoparticle size after i.v. injection of colloidal gold in mice, smaller particles (10-50 nm) were found to disperse quickly to almost all tissues, mainly accumulating in the liver, lungs, spleen, and kidneys at 24 h post injection. Larger particles (100-200 nm) were found in the liver, lungs, spleen, and kidneys, but they were not as widely dispersed into other tissues as were the smaller particles. These studies concluded a size-dependent distribution and potential toxicity of smaller (< 50 nm) gold nanoparticles [31, 42].

Surface Plasmon

Gold at the nanoscale can appear red, blue, green, or brown according to their size and shape (Figure 1). These colors arise as a result from interaction of band electrons in the metallic nanoparticles with the incident light. Furthermore, the optical cross-sections of AuNPs are typically four or five orders of magnitude higher than those of conventional dyes [43]. That is, AuNPs with a diameter of 40 nm have a calculated molar absorption coefficient (ϵ) of $\sim 7.7 \times 10^9 \text{ M}^{-1} \text{ cm}^{-1}$ at a wavelength maximum around 530 nm, four orders of magnitude larger than the extinction coefficient for rhodamine 6G ($\epsilon = 1.2 \times 10^5 \text{ M}^{-1} \text{ cm}^{-1}$ at 530 nm). Another interesting property of AuNP SPR (surface plasmon resonance) is its sensitivity to the local refractive index/dielectric constant of the environment surrounding the nanoparticle surface [44]. The nanosphere plasmon resonance shifts to higher wavelengths with increasing refractive index of the medium. This phenomenon has been explored in the sensing of biomolecular analytes by monitoring a change in the SPR wavelength with the occurrence of an adsorption/binding event at the surface of silver or gold nanoparticles [44]. The nanoparticle SPR can also be redshifted by the self-assembly or aggregation of particles [45].

The intense surface-plasmon-enhanced scattering from gold nanoparticles makes them promising as optical probes and labels for imaging-based detection of cancers.

Depending on the gold nanoparticle's size, shape, and surrounding medium, a relatively narrow range of frequencies of incident light induce resonant conduction band electron oscillation. This resonance is called the localized surface plasmon resonance (LSPR), which occurs in the visible and near-infrared regime of the spectrum for gold nanoparticles, depending on their shape and size [46]. In the case of spherical nanoparticles, a single „plasmon“ band is observed in the visible region. But, when the nanoparticles have an anisotropic shape (1D nanoparticle), two plasmon bands occur as a result of electron oscillation along the two axes [47]. The transverse „plasmon band of gold nanorods occurs at ~ 520 nm, corresponding to electron oscillation along the short axis of the particle; the longitudinal „plasmon band at longer wavelengths is governed by the nanorods' length/width ratio (aspect ratio) (Figure 2). The wavelength of the longitudinal band can be tuned by controlling the dimensions of the gold nanorods. Thus, it is possible to prepare nanoparticles which absorb in the biological „water window“ of ~ 800 – 1200 nm. In this wavelength range, few chromophores absorb, background fluorescence is low, water does not absorb, and thus light can penetrate deeper in biological tissues [48]. These 1D nanoparticles are of clinical significance and contribute to the popularity of gold and

silver nanorods for biomedical therapeutic/imaging agents [49]. The strong light extinction (absorption and scattering) of gold nanorods has been employed in various biomedical imaging applications. Furthermore, the dependence of the plasmon band position on the degree of aggregation of the nanoparticles and on the dielectric constant of the local environment forms the basis for chemical sensing with gold nanoparticles[50].

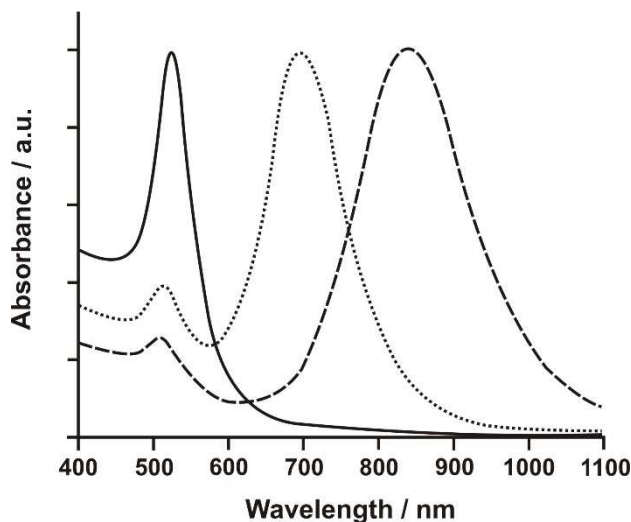


Figure 2: Surface Plasmon Absorption Spectra of Gold Spherical Nanoparticles (Solid Line) and Nanorods of Different Aspect Ratios (Dotted and Dashed Lines), Showing the Sensitivity of the Strong Longitudinal Band to the Aspect Ratios of the Nanorods

There are two current approaches, both of which produce structures with two tunable plasmon resonances: cylindrical nanoparticles, or nanorods, and dielectric core-shell nanoparticles, or nanoshells [51]. We can grow a thin, homogeneous gold shell around a hematite particle to create a layered nanostructure with a shape known as a prolate spheroid. Nanorods are special particles because they truly are hybrids, combining the tunable plasmon properties of nanoshells with the high field focusing shape of nanorods in a single particle. The results indicate that plasmon tunability arising from variation in the shell thickness is far more geometrically sensitive than that arising from variation of the length of the nanorod.

Nanoshells can be composed of various material (e.g., silica) core surrounded by a thin gold shell, and will absorb energy (heat up) when exposed to the appropriate wavelength of light. The near-infrared characteristics were chosen because absorption by tissues is minimal and penetration of the light is optimal at this wavelength. The nanoshells can accumulate in implanted tumors. This can occur as most tumor vasculature is “leaky” and will allow nanosized particles to penetrate into the tumor while normal tissue or organs are not affected. The tumors are then illuminated with a near-infrared diode laser to heat the tumor and cause cellular destruction. By this protocol all the tumors were ablated, and the mice remained tumor-free for many months. In appropriate settings, thermal ablation methods could be used to replace surgical resection of tumors, and targeted therapies and immunotherapy as a substitute for toxic chemotherapy. The nanomedicinal methods being developed have a good chance of achieving this goal with much less damage to normal tissue than existing therapeutic protocols [52].

In addition to enhance all the radiative properties such as absorption and scattering, the field enhances the Raman scattering of adjacent molecules because the Raman intensity is directly proportional to the square of the field intensity imposed on the molecules [53]. This phenomenon is termed as surface enhanced Raman scattering (SERS). The induced

field for the Raman enhancement is determined by the particle size, shape, composition and particle relative orientation and distance [54, 55]. This indicates that for large Raman enhancement, asymmetric AuNPs, which gives high curvature surface, are more favorable due to the “lightening-rod” effect. As demonstrated by Nikoobakht et al., enhancement factors on the order of 10^4 – 10^5 were observed for adsorbed molecules on the nanorods while no such enhancement was observed on nanospheres under similar condition [56]. Huang et al. applied SERS by gold nanorods to diagnose cancer cells from normal cells [57]. Gold nanorods are conjugated to anti-EGFR antibodies and then specifically bound to human oral cancer cells. Compared to HaCat normal cells, the anti-EGFR antibodies as well as cellular components in the surface plasmon field of the gold nanorods on the cancer cell surface are found to give a Raman spectrum which is greatly enhanced due to the high surface plasmon field of aggregated nanorod assembly and sharp due to a homogenous environment. The polarization property of the SERS of the molecules monitored by the strongest band of the cetyltrimethylammonium bromide (CTAB) capping molecules indicates that gold nanorods are assembled and aligned on the cancer cell surface and thus giving much stronger Raman enhancement. These observed properties can be used as molecular diagnostic signatures for cancer cells. Although traditional Raman has also been used to diagnose abnormal breast cancer tissue [58], SERS is more advantageous because it greatly enhances detection sensitivity and decreases signal acquisition time (Figure 3).

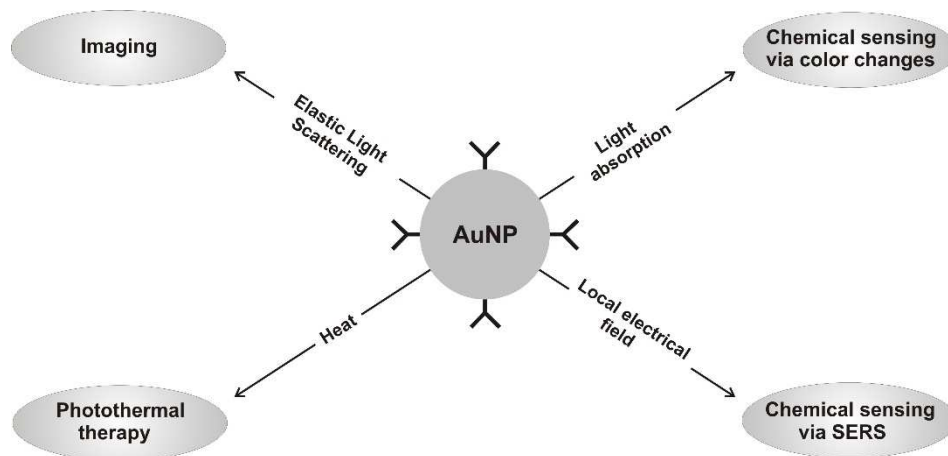


Figure 3: Schematic Showing the Physical Events that Occur as a Result of Satisfying the Localized Surface Plasmon Resonance Condition, with the Corresponding Applications [47]

Cancer Cell Imaging by Gold Nanoparticle Bioconjugates

Many nanomaterials are functionalized on the surface to increase blood circulation, make them more biocompatible, and for targeted therapy. While functionalization has shown promise in many applications, functional groups added to the surface can potentially interact with biological components, alter biological function, and allow passage of nanomaterials that would not normally be taken up by certain cells. The flavonoid functionalization, for example, helps for reducing the toxicity in the host and offers only synergic effect in case of the functionalized AuNP. Thus, this flavonoid-conjugated AuNP disturbs and destroys the cell externally. Figure 4 shows the pictorial representation of shape-dependent anti-cancer effect of gold nanoparticles. The irregularly shaped nanoparticles can move easily in between the abnormally high and irregularly spread neoplastic cells compared to polyshaped or roughly spherical ones; it is reasonable to infer that these special unpredictable amoebic shaped is having better anti-proliferative effect. Particle size can also affect the mode of endocytosis, cellular uptake, and the efficiency of particle processing in the endocytic pathway [59]. Some studies of non-phagocytic cellular uptake of latex spheres have demonstrated slower uptake and processing of large spheres (>200 nm) relative to small ones (50 and 100 nm) [60]. Gold nanomaterials can be found in many different

shapes, especially as spherical clusters and nanorods. Along with size, Chithrani et al. studied the effect of shape on the cellular uptake of gold nanoparticles. They concluded that both nanorods (74×14 nm) and spherical particles (74 and 14 nm) are taken up by cells; however, nanorod uptake is slower relative to spherical particles in HeLa cells [24]. Wang et al. further concluded that nanorods are more cytotoxic than spherical gold nanomaterials to human HeCaT keratinocytes [61]. Although both studies concluded differences between spherical particles and nanorods, both Chithrani et al. and Wang et al. suggested that the more important difference in cellular uptake rates and cytotoxicity was the use of different chemistries to stabilize the gold nanomaterials. Although aggregation of gold nanorods has been shown intercellularly, nanospheres also show aggregation without causing cytotoxicity [61, 62].

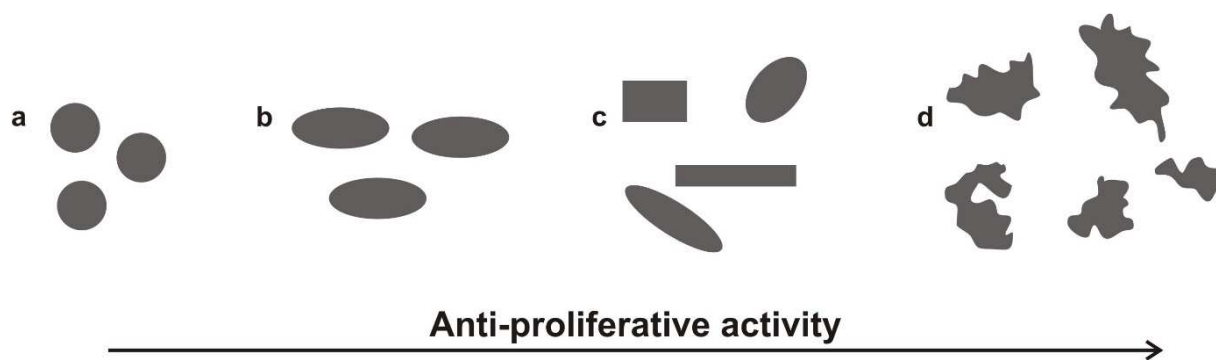


Figure 4: Shape-Dependent Anti-Proliferative Activity of Gold Nanoparticles from Spherical (a) to Irregular (d) [63]

Degradability of the material is an important component of acute and long-term toxicity. Nondegradable nanomaterials can accumulate in organs and also intracellularly where they can cause detrimental effects to the cell, similar to that of lysosomal storage diseases [64]. In contrast, biodegradable nanomaterials can lead to unpredicted toxicity due to unexpected toxic degradation products [65]. Nanomaterials may contain transition metals or other metal compounds with known toxicity that are “masked” for instance by functionalization. Degradation of this material may release toxins to the biological milieu, leading to free radical formation and resulting in cellular damage [65].

The addition of targeting ligands that provide specific nanoparticle–cell surface interactions can play a vital role in the ultimate location of the nanoparticle. For example, nanoparticles can be targeted to cancer cells if their surfaces contain moieties such as small molecules, peptides, proteins or antibodies. These moieties can bind with cancer cell surface receptor proteins, such as transferrin receptors, that are known to be increased in number on a wide range of cancer cells [66]. These targeting ligands enable nanoparticles to bind to cell-surface receptors and enter cells by receptor-mediated endocytosis. Further works comparing non-targeted and targeted nanoparticles (lipid-based [67] or polymer-based [68] have shown that the primary role of the targeting ligands is to enhance cellular uptake into cancer cells rather than increasing the accumulation in the tumour.

The ability of gold nanoparticles developed from clove extract inhibit proliferation of HEK-293, HeLa, and HT-29 cell line was estimated by its observed effect on the growth of the cells [63]. The growth of the untreated (control) and treated HEK-293, HeLa, and HT-29 cell line after incubation was followed. The observation of HEK-293, HeLa, and HT-29 cells showed that most of the cells were attached in the culture containing $20 \mu\text{g/mL}$ of AuNPs functionalized with clove moieties. The cells were viable and adhered to the bottom of the well after 48 h of treatment, although a large proportion of the cells were found in isolated condition. Cells of all cancer cell lines are shrunken and isolated condition

after 48 h of incubation. AuNP synthesized from clove, causes 50% cell death in all human cancer cell lines tested. The clove extract-mediated AuNP has been proven to inhibit the proliferation of three cancer cell lines out of four that were tested at a strong IC_{50} value ($<20 \mu\text{g/mL}$). These nanoparticles were not active ($IC_{50} > 30 \mu\text{g/mL}$) against K-562.

The freely water-soluble flavonoids present in the guava leaf (Gua) and clove (Clo) buds solution that could have been adsorbed on the surface can stimulate or suppress the immune system due to the presence of $-\text{OH}$ groups. Presence of such phenolic moieties may be assumed to have synergic effect for the anti-proliferative activities of these bio-adsorbed metal nanoparticles [69]. These shape-dependent properties of AuNP have different behaviors and make them suitable for therapeutic utilization [70]. AuNPs of certain non-regular shapes can readily be adsorbed to the surfaces of the biomolecules which show higher surface plasmon resonance and will have a greater contrast effect than those of photothermal dyes that are used regularly in detection of cancer cells [71]. Here, the bio-detection sensitivity and biocompatibility parameters become very important. The bio-detection sensitivity of nanoparticles often is associated with their physical and chemical properties, which in turn depend on the shape of the particles [72]. Nanoparticles with different dimensions have been applied widely to detect biological molecules. Colloidal AuNPs are used to detect specific DNA sequences and single-base mutations in a homogeneous format. AuNPs synthesized with biological base are interesting, predominantly because they exhibit the best compatibility with biomolecules. But, bio-detection sensitivity derived from spherical nanoparticles is not strong enough to trace the interaction of biomolecules [73]. Looking into all these aspects, it is reasonable to infer that the biosynthesis of irregular-shaped nanoparticles hopefully might reach this aim because they display novel properties and may improve biological detection sensitivity greatly (Figure 2). The shape of the noble nanoparticle will also play important role as an anti-cancer agent. Raghunandan et al. have speculated on the possible mechanisms that govern shape-dependent extracellular effect of nanoparticles [63].

AuNP-Clo conjugate proved to possess antiproliferative properties against all the cancer cell lines tested. The prominent anti-proliferative effect of functionalized AuNP on HEK-293, HeLa, and HT-29 cancer cell lines, as revealed by its IC_{50} based on XTT assay was found to be ~ 19.88 , ~ 20.05 , ~ 20.12 , and ~ 28.56 , respectively. IC_{50} of AuNP-Clo was specifically less significant on Vero cell line, i.e., ~ 55.3 . Therefore, it can be said that AuNP-Clo is a promising anti-cancer "lead". AuNP-Gua conjugate has shown activity against HEK-293 but the $IC_{50} > 30 \mu\text{g/mL}$. These are devoid of anti-proliferative activity against other three cell lines. AuNPs developed with cow urine as a reducing agent have shown activity against HeLa, HEK-293, and HT-29 at $30 \mu\text{g/mL}$. Though the inhibitory effect is higher than that of AuNP-Clo, but looking in to the beneficial effects of cow urine, the AuNPs synthesized with using cow urine as a reducing medium can be a promising anti-cancer agent. Poly-shaped nanoparticles synthesized using guava extract has shown cytotoxic effect on HEK-293 and the IC_{50} . Functionalized AgNP using other different plant extract and bio-excretory have not shown any cytotoxic effect even at $30 \mu\text{g/mL}$. This also proves that the adsorbed bio-moieties alone are devoid of cytotoxic effect at that concentration.

CONCLUSIONS

Targeted gold nanoparticles have provided an effective platform for imaging and detection of cancer and a better and more specific delivery of cancer therapeutics. These targeted nanoparticles would be able to detect cancer cells, visualize their location in the body, deliver drugs to these cells only, circumvent drug resistance, kill cancer cells while sparing normal cells with minimal side effects, monitor treatment effects in real time, and provide feedback whether the patients respond well to the treatments to stop the treatment in time. The role and scope of targeted nanoparticles for drug

delivery in cancer therapy is growing, and the development of effective multifunctional targeted nanoparticles will not be far in the future. The first of these creative treatment methods have made it to the clinic and hopefully are well on their way to improving the length and quality of life for cancer patients. However, there is a great deal more that can be done to treat and perhaps prevent advanced cancer by treating it in as early a stage as possible. This will require superior detection and targeting methods which many of the researchers mentioned here will undoubtedly pursue and hopefully achieve. There has been a sharp growth in the pace of discovery and development of targeted nanoparticles over the past few years. Current preclinical data support the hypothesis that targeted NPs can provide the means to deliver drugs at a prolonged rate to specific cancer targets. Once optimized, these targeted NPs will provide the improved treatment options that are so urgently sought for cancer. In essence, all drug molecules can be considered as nanoengineered structures. Tumor destruction via the use of nanoparticles for thermal ablation is also being examined and shows promise as a nonsurgical method for tumor removal. This will allow the creation of simple approach for use in the oncology clinic. Due to the complexity of cancers, a combination of approaches will likely be needed for the effective elimination of all tumor cells.

ACKNOWLEDGEMENTS

Study was supported by VEGA-2/0040/14 and -2/0152/13 projects.

REFERENCES

1. Kim, S.; Kim, J.H.; Jeon, O.; Kwon, I.C.; Park, K. Engineered polymers for advanced drug delivery. *Eur. J. Pharm. Biopharm.*, **2009**, *71*, 420-430.
2. Maeda, H.; Matsumura, Y. Tumoritropic and lymphotropic principles of macromolecular drugs. *Crit. Rev. Ther. Drug*, **1989**, *6*, 193-210.
3. Matsumura, Y.; Maeda, H. A new concept of macromolecular therapies in cancer chemotherapy: mechanism of tumortropic accumulation of proteins and the antitumor agent SMANCS. *Cancer Res.*, **1986**, *6*, 6387-6392.
4. Dreher, M.R.; Liu, W.; Michelich, C.R.; Dewhirst, M.W.; Yuan, F.; Chilkoti, A. Tumor vascular permeability, accumulation, and penetration of macromolecular drug carriers. *J. Natl Cancer Inst.*, **2006**, *98*, 335-344.
5. Nomura, T.; Koreeda, N.; Yamashita, F.; Takakura, Y.; Hashida, M. Effect of particle size and charge on the disposition of lipid carriers after intratumoral injection into tissue-isolated tumors. *Pharm Res.*, **1998**, *15*, 128-132.
6. Hu-Lieskovan, S.; Heidel, J.D.; Bartlett, D.W.; Davis, M.E.; Triche, T.J. Sequence-specific knockdown of EWS-FLI1 by targeted, nonviral delivery of small interfering RNA inhibits tumor growth in a murine model of metastatic Ewing's sarcoma. *Cancer Res.*, **2005**, *65*, 8984-8992.
7. Sholley, M.M.; Ferguson, G.P.; Seibel, H.R.; Montour, J.L.; Wilson, J.D. Mechanisms of neovascularization. Vascular sprouting can occur without proliferation of endothelial cells. *Lab. Invest.*, **1984**, *51*, 624-634.
8. Folkman, J. *Angiogenesis*. in: E. Braunwald, A.S. Fauci, D.L. Kasper et al, (Eds.) Harrison's textbook of internal medicine. 15th ed. McGraw-Hill, New York (NY); **2001**, pp. 517-530.
9. Folkman, J. Angiogenesis: an organizing principle for drug discovery? *Nat. Rev. Drug. Discov.*, **2007**, *6*, 273-286.
10. Brannon-Peppas, L.; Blanchette, J.O. Nanoparticle and targeted systems for cancer therapy. *Adv. Drug. Deliv.*

- Rev.*, **2004**, *56*, 1649-1659.
11. Folkman, J. Tumor angiogenesis: therapeutic implications. *N. Engl. J. Med.*, **1971**, *285*, 1182-1186.
 12. Hillen, F.; Griffioen, A.W. Tumour vascularization: sprouting angiogenesis and beyond. *Cancer Metastasis Rev.*, **2007**, *26*, 489-502.
 13. Heldin, C.H.; Rubin, K.; Pietras, K.; Ostman, A. High interstitial fluid pressure - an obstacle in cancer therapy. *Nat. Rev. Cancer*, **2004**, *4*, 806-813.
 14. Ikeda, Y.; Hayashi, I.; Kamoshita, E.; Yamazaki, A.; Endo, H.; Ishihara, K.; Yamashina, S.; Tsutsumi, Y.; Matsubara, H.; Majima, M. Host stromal bradykinin B2 receptor signaling facilitates tumor-associated angiogenesis and tumor growth. *Cancer Res.*, **2004**, *64*, 5178-5185.
 15. Maeda, H.; Wu, J.; Sawa, T.; Matsumura, Y.; Hori, K. Tumor vascular permeability and the EPR effect in macromolecular therapeutics: a review. *J. Control. Release*, **2000**, *65*, 271-284.
 16. Yuan, F.; Dellian, M.; Fukumura, D.; Leunig, M.; Berk, D.A.; Torchilin, V.P.; Jain, R.K. Vascular permeability in a human tumor xenograft: molecular size dependence and cutoff size. *Cancer Res.*, **1995**, *55*, 3752-3756.
 17. Maeda, H.; Bharate, G.Y.; Daruwalla, J. Polymeric drugs for efficient tumor-targeted drug delivery based on EPR-effect. *Eur. J. Pharm. Biopharm.*, **2009**, *71*, 409-419.
 18. Wang, J.; Sui, M.; Fan, W. Nanoparticles for tumor targeted therapies and their pharmacokinetics. *Current Drug Metabolism.*, **2010**, *11*, 129-141.
 19. Noguchi, Y.; Wu, J.; Duncan, R.; Strohalm, J.; Ulbrich, K.; Akaike, T.; Maeda, H. Early phase tumor accumulation of macromolecules: a great difference in clearance rate between tumor and normal tissues. *Cancer Science*, **1998**, *89*, 307-314.
 20. Li, S.D.; Huang, L. Pharmacokinetics and biodistribution of nanoparticles. *Mol. Pharm.*, **2008**, *5*, 496-504.
 21. Davis, M.E.; Chen, Z.G.; Shin, D.M. Nanoparticle therapeutics: an emerging treatment modality for cancer. *Nat. Rev. Drug Discov.*, **2008**, *7*, 771-782.
 22. Turner, M.; Golovko, V.B.; Vaughan, O.P.H. Selective oxidation with dioxygen by gold nanoparticle catalysts derived from 55-atom clusters. *Nature*, **2008**, *454*, U31-981.
 23. Tsoli, M.; Kuhn, H.; Brandau, W.; Esche, H.; Schmid, G. Cellular uptake and toxicity of Au(55) clusters. *Small*, **2005**, *1*, 841-844.
 24. Chithrani, B.D.; Ghazani, A.A.; Chan, W.C.W. Determining the size and shape dependence of gold nanoparticle uptake into mammalian cells. *Nano Lett.*, **2006**, *6*, 662-668.
 25. Gao, H.J.; Shi, W.D.; Freund, L.B. Mechanics of receptor-mediated endocytosis. *Proc. Natl. Acad. Sci. USA*, **2005**, *102*, 9469-9474.
 26. Verma, A.; Uzun, O.; Hu, Y.H. Surface-structure-regulated cell-membrane penetration by monolayer-protected nanoparticles. *Nat. Mater.*, **2008**, *7*, 588-595.

27. Alkilany, A.M.; Nagaria, P.K.; Hexel, C.R.; Shaw, T.J.; Murphy, C.J.; Wyatt, M.D. Cellular uptake and cytotoxicity of gold nanorods: molecular origin of cytotoxicity and surface effects. *Small*, **2009**, *5*, 701-708.
28. Nativo, P.; Prior, I.A.; Brust, M. Uptake and intracellular fate of surface-modified gold nanoparticles. *ACS Nano*, **2008**, *2*, 1639-1644.
29. Datar, R.H.; Richard, J.C. Nanomedicine: concepts, status and the future. *Medical Innovation & Business*, **2010**, *2*, 6-17.
30. Kim, C.; Ghosh, P.; Rotello, V.M. Multimodal drug delivery using gold nanoparticles. *Nanoscale*, **2009**, *1*, 61-67.
31. De Jong, W.H.; Hagens, W.I.; Krystek, P.; Burger, M.C.; Sips, A.J.A.M.; Geertsma, R.E. Particle size-dependent organ distribution of gold nanoparticles after intravenous injection. *Biomaterials*, **2008**, *29*, 1912- 1919.
32. Storm, G.; Belliot, S.O.; Daemen, T.; Lasic, D. Surface modification of nanoparticles to oppose uptake by the mononuclear phagocyte system. *Adv. Drug Del. Rev.*, **1995**, *17*, 31- 48.
33. Hirsch, L.R.; Gobin, A.M.; Lowery, A.R.; Tam, F.; Drezek, R.A.; Halas, N.J.; West, J.L. Metal nanoshells. *Ann. Biomed. Eng.*, **2006**, *34*, 15-22.
34. Arias, J. L.; Gallardo, V.; Linares-Molinero, F.; Delgado, A.V. Distribution of drug to the cancer cells, limiting systemic drug concentrations. *J. Colloid Interface Sci.*, **2006**, *299*, 599-607.
35. Deutscher, S. L. Phage display in molecular imaging and diagnosis of cancer. *Chem. Rev.*, **2010**, *110*, 3196-3211.
36. Farokhzad, O.C.; Jon, S.; Khademhosseini, A.; Tran, T.N.; Lavan, D.A. Nanoparticle-aptamer bioconjugates: a new approach for targeting prostate cancer. *Cancer Res.*, **2004**, *64*, 7668-7672.
37. Bagalkot, V.; Farokhzad, O.C.; Langer, R.; Jon, S. Nanoparticle therapeutics for prostate cancer treatment. *Angew. Chem. Int. Ed.*, **2006**, *45*, 8149-8152.
38. Jain, P.K.; El-Sayed, I.H.; El-Sayed, M.A. Au nanoparticles target cancer. *Nanotoday*, **2007**, *2*, 18-29.
39. Schmid, G. The relevance of shape and size of Au55 clusters. *Chem. Soc. Rev.*, **2008**, *337*, 1909-1930.
40. Pan, Y.; Neuss, S.; Leifert, A.; Fischler, M.; Wen, F.; Simon, U.; Schmid, G.; Brandau, W.; Jahnke-Dechent, W. Size-dependent cytotoxicity of gold nanoparticles. *Small*, **2007**, *3*, 1941-1949.
41. Chithrani, B.D.; Chan, W.C.W. Elucidating the mechanism of cellular uptake and removal of proteincoated gold nanoparticles of different sizes and shapes. *Nano Lett.*, **2007**, *7*, 1542-1550.
42. Sonavane, G.; Tomoda, K.; Makino, K. Biodistribution of colloidal gold nanoparticles after intravenous administration: effect of particle size. *Colloids Surf. B Biointerfaces*, **2008**, *66*, 274-280.
43. Jain, P.K.; Lee, K.S.; El-Sayed, I.H.; El-Sayed, M.A. The influence of size, shape, and dielectric environment. *J. Phys. Chem. B*, **2006**, *110*, 7238-7248.
44. Zhao, J.; Zhang, X.; Yonzon, C.R.; Haes, A.J.; Van Duyne, R.P. Plasmonic Au/Co/Au nanosandwiches. *J. Fluorescence*, **2004**, *14*, 355-367.
45. Jain, P.K.; Eustis, S.; El-Sayed, M.A. Plasmon coupling in nanorod. *J. Phys. Chem. B*, **2006**, *110*, 18243-18253.

46. Kelly, K.L.; Coronado, E.; Zhao, L.L.; Schatz, G.C. The optical properties of metal nanoparticles: the influence of size, shape, and dielectric environment. *J. Phys. Chem. B*, **2003**, *107*, 668-677.
47. Alkilany, A.M.; Murphy, C.J. Toxicity and cellular uptake of gold nanoparticles. *J. Nanopart. Res.*, **2010**, *12*, 2313-2333.
48. Weissleder, R. A clearer vision for in vivo imaging. *Nat Biotechnol.*, **2001**, *19*, 316-317.
49. Jain, P.K.; Huang, X.H.; El-Sayed, I.H.; El-Sayed, M.A. Noble metals on the nanoscale: optical and photothermal properties and some applications in imaging, sensing, biology, and medicine. *Acc. Chem. Res.*, **2008**, *41*, 1578-1586.
50. Murphy, C.J.; Gole, A.M.; Hunyadi, S.E. Chemical sensing and imaging with metallic nanorods. *Chem. Commun.*, **2008**, *5*, 544-557.
51. Wang, H.; Brandl, D.W.; Le, F.; Nordlander, P.; Halas, N.J. Nanorice: a hybrid nanostructure. *Nano Lett.*, **2006**, *6*, 827-832.
52. Kawasaki, E.S.; Player, A. Nanotechnology, nanomedicine, and the development of new, effective therapies for cancer. *Nanomedicine: Nanotechnology, Biology, and Medicine*, **2005**, *1*, 101- 109.
53. Kneipp, K.; Kneipp, H.; Itzkan, I.; Dasari, R.R.; Feld, M.S. Surfaceenhanced Raman scattering and biophysics. *J. Phys. Condens. Mater.*, **2002**, *14*, R597-624.
54. Hao, E.; Schatz, G.C. Electromagnetic fields around silver nanoparticles and dimers. *J. Chem. Phys.*, **2004**, *120*, 357-366.
55. Hao, E.; Schatz, G.C.; Hupp, J.T. Synthesis and optical properties of anisotropic metal nanoparticles. *J. Fluor.*, **2004**, *14*, 331-341.
56. Nikoobakht, B.; Wang, J.; El-Sayed, M.A. Surface-enhanced Raman scattering of molecules adsorbed on gold nanorods: off-surface plasmon resonance condition. *Chem. Phys. Lett.*, **2002**, *366*, 17-23.
57. Huang, X.; El-Sayed, I.H.; Qian, W.; El-Sayed, M.A. Cancer cells assemble and align gold nanorods conjugated to antibodies to produce highly enhanced, sharp and polarized surface Raman spectra: a potential cancer diagnostic marker. *Nano Lett.*, **2007**, *7*, 1591-1597.
58. Haka, A.S.; Shafer-Peltier, K.E.; Fitzmaurice, M.; Crowe, J.; Dasari, R.R.; Feld, M.S. Diagnosing breast cancer by using Raman spectroscopy. *Proc. Natl. Acad. Sci. USA*, **2005**, *102*, 12371-12376.
59. Lanone, S.; Boczkowski, J. Biomedical applications and potential health risks of nanomaterials: molecular mechanisms. *Curr. Mol. Med.*, **2006**, *6*, 651-663.
60. Rejman, J.; Oberle, V.; Zuhorn, I.S.; Hoekstra, D. Size-dependent internalization of particles via the pathways of clathrin- and caveolae-mediated endocytosis. *Biochem. J.*, **2004**, *377*, 159-169.
61. Wang, S.; Lu, W.; Tovmachenko, O.; Rai, U.S.; Yu, H.; Ray, P.C. Challenge in understanding size and shape dependent toxicity of gold nanomaterials in human skin keratinocytes. *Chem. Phys. Lett.*, **2008**, *463*, 145-149.
62. Connor, E.E.; Mwamuka, J.; Gole, A.; Murphy, C.J.; Wyatt, M.D. Gold nanoparticles are taken up by human cells

- but do not cause acute cytotoxicity. *Small*, **2005**, *1*, 325-327.
63. Raghunandan, D.; Ravishankar, B.; Sharanbasava, G.; Mahesh, D.B.; Harsoor, V.; Yalagatti, M.S.; Bhagawanraju, M.; Venkataraman, A. Anti-cancer studies of noble metal nanoparticles synthesized using different plant extracts. *Cancer Nanotechnol.*, **2011**, *2*, 57-65.
 64. Garnett, M.C.; Kallinteri, P. Nanomedicines and nanotoxicity: some physiological principles. *Occup. Med.*, **2006**, *56*, 307-311.
 65. Fischer, H.C.; Chan, W.C.W. Nanotoxicity: the growing need for in vivo study. *Curr. Opin. Biotechnol.*, **2007**, *18*, 565-571.
 66. Gatter, K.C.; Brown, G.; Trowbridge, I.S.; Woolston, R.E.; Mason, D.Y. Transferrin receptors in human tissues: their distribution and possible clinical relevance. *J. Clin. Pathol.*, **1983**, *36*, 539-545.
 67. Kirpotin, D.B.; Drummond, D.C.; Shao, Y.; Shalaby, M.R.; Hong, K.; Nielsen, U.B.; Marks, J.D.; Benz, C.C.; Park, J.W. Antibody targeting of longcirculating lipidic particles does not increase tumor localization but does increase internalization in animal models. *Cancer Res.*, **2006**, *66*, 6732-6740.
 68. Bartlett, D.W.; Su, H.; Hildebrandt, I.J.; Weber, W.A.; Davis, M.E. Impact of tumor-specific targeting on the biodistribution and efficacy of siRNA nanoparticles measured by multimodality in vivo imaging. *Proc. Natl Acad. Sci. USA*, **2007**, *104*, 15549-15554.
 69. Lee, S.; Park, H. Anticancer activity of guava (*Psidium guajava* L.) branch extracts against HT-29 human colon cancer cells. *Journal of Medicinal Plants Research*, **2010**, *4*, 891-896.
 70. Sperling, R.A.; Gil, P.R.; Zhang, F.; Zanella, M.; Parak, W.J. Biological applications of gold nanoparticles. *Chem. Soc. Rev.*, **2008**, *37*, 1896-1908.
 71. Giljohann, D.A.; Seferos, D.S.; Daniel, W.L.; Massich, M.D.; Patel, P.C.; Mirkin, C.A. Gold nanoparticles for biology and medicine. *Nanotechnology, Science and Applications*, **2010**, *49*, 3280-3294.
 72. Hu, J.; Wang, Z.; Li, J. Gold nanoparticles with special shapes: controlled synthesis, surface-enhanced raman scattering, and the application in bio-detection. *Sensors*, **2007**, *7*, 3299-3311.
 73. Orendorff, C.J.; Sau, T.K.; Murphy, C. Shape-dependent plasmonresonant gold nanoparticles. *Small*, **2006**, *2*, 636-639.